Femtosecond Spectroscopic Observations of Initial Intermediates in the Photocycle of the Photoactive Yellow Protein from *Ectothiorhodospira halophila*

Savitha Devanathan,* Andrew Pacheco,# Laszlo Ujj,# Michael Cusanovich,* Gordon Tollin,* Su Lin,§ and Neal Woodbury§

Departments of *Biochemistry and #Chemistry, University of Arizona, Tucson, Arizona 85721; and §Department of Chemistry and Biochemistry, Arizona State University, Tempe, Arizona USA

ABSTRACT Femtosecond time-resolved absorbance measurements were used to probe the subpicosecond primary events of the photoactive yellow protein (PYP), a 14-kD soluble photoreceptor from *Ectothiorhodospira halophila*. Previous picosecond absorption studies from our laboratory have revealed the presence of two new early photochemical intermediates in the PYP photocycle, I_0, which appears in $\leq$3 ps, and $I_0^{\ddagger}$, which is formed in 220 ps, as well as stimulated emission from the PYP excited state. In the present study, kinetic measurements at two excitation wavelengths (395 nm and 460 nm) on either side of the PYP absorption maximum (446 nm) were undertaken using 100-fs pump and probe pulses. Global analysis over a range of probe wavelengths yielded time constants of 1.9 ps for the photochemical formation of the I_0 intermediate via the PYP excited state, and 3.4 ps for the repopulation of the ground state from the excited state. In addition to these pathways, 395 nm excitation also initiated an alternative route for PYP excitation and photochemistry, presumably involving a different excited electronic state of the chromophore. No photochemical intermediates formed before I_0 were observed. Based on these data, a quantum yield of 0.5–0.6 for I_0 formation was determined. The structural and mechanistic aspects of these results are discussed.

INTRODUCTION

Photoactive yellow protein (PYP) is a biomolecular photoreceptor found in the cytosol of the halophilic purple phototrophic bacterium *Ectothiorhodospira halophila* and related bacterial species (Meyer, 1985; Meyer et al., 1987, 1990). The chromophore responsible for perception of light and the resultant yellow color of this protein is a *p*-hydroxycinnamic acid molecule covalently tethered via a thiol ester linkage to Cys-69 (Baca et al., 1994). The absorbed light energy is transduced by PYP through a photocycle involving several intermediate species with lifetimes ranging from picoseconds to milliseconds (Meyer et al., 1987; Ujj et al., 1998), presumably to mediate negative phototaxis (Sprenger et al., 1993).

Two new early intermediates, I_0 [time constant (τ) for formation (defined as $1/k$) $\leq$ 3 ps] and $I_0^{\ddagger}$ ($\tau_{formation}$ = 220 ps), in this photocycle were recently characterized by picosecond pump-probe spectroscopy (Ujj et al., 1998), in addition to the previously known microsecond and millisecond intermediates, I_1 (τ_{decay} = 140 μs) and I_2 (τ_{decay} = 97 ms), characterized by nanosecond time-resolved spectroscopy (Meyer et al., 1987; Genick et al., 1997a). In contrast to our observations of the formation and decay of the I_0 species, data recently reported using femtosecond spectroscopy (Baltuška et al., 1997) were interpreted in terms of the formation of two kinetically resolved species with time constants τ = 0.7 and τ = 3.6 ps, which were incorrectly attributed to the formation of the I_1 intermediate, which is actually produced with a time constant of 3 ns (Ujj et al., 1998). Fluorescence upconversion measurements also have characterized emission processes that occur in the 0.6–3.6-ps time scales (Chosrowjan et al., 1997).

The above-noted inconsistency in the assignment of photochemical intermediate formation times for I_0 and I_1 has stimulated us to extend our previous picosecond kinetic characterization (Ujj et al., 1998) to the femtosecond time scale in order to further clarify the early stages of the PYP photocycle. To do this, we have used a transient absorption apparatus with ~100 fs time resolution. These measurements have confirmed the formation of I_0 and $I_0^{\ddagger}$ within a few hundred picoseconds after excitation, and have resolved the kinetics of ground state bleaching and repopulation in the blue spectral region (430–465 nm) as well as stimulated emission in the longer wavelength regime (500–550 nm) occurring between −1 and 7 ps. The results have resolved the kinetics of formation of the I_0 transient species (τ = 1.9 ps, $k = 0.54 \times 10^{12}$ s^{-1}; see below) formed during the decay of the PYP excited state (P*), and the kinetics of the repopulation of the ground state from P* (τ = 3.4 ps, $k = 0.29 \times 10^{12}$ s^{-1}). No additional photochemical intermediates were detected before the formation of I_0. The data also demonstrate that excitation on the blue side (395 nm) and on the red side (460 nm) of the 446 nm absorption band of PYP produce excited states that have somewhat different properties before the formation of I_0.

EXPERIMENTAL

Sample preparation

Recombinant PYP with purity index 0.45 (OD 278/446 nm) was prepared according to a previously published procedure (Devanathan et al., 1997).

Received for publication 5 January 1999 and in final form 28 April 1999.

Address reprint requests to Dr. Gordon Tollin, Dept. of Biochemistry, University of Arizona, Tucson, AZ 85721. Tel.: 520-621-3447; Fax: 520-621-9288; E-mail: gtollin@u.arizona.edu.

0006-3495/99/08/1017/07 $2.00

Four ml of a PYP solution (1.4 OD/cm) in 20 mM Tris-Cl buffer at pH 7.0 was rotated at 2 rpm in a 2-mm optical pathlength sample wheel through the path of the laser pulses to prevent accumulation and excitation of the long-lived PYP photointermediates.

Femtosecond transient absorption (FTA) spectroscopy

Transient absorption difference spectra were obtained using a pump-probe apparatus. Femtosecond pulses were provided by a Ti:Sapphire regenerative amplifier (CPA-1000, Clark-MXR, Dexter, MI) pumped by a diode-pumped solid-state laser (Millennia, Spectra-Physics, Mountain View, CA). The output pulses from the CPA-1000 were at a wavelength of 790 nm with a pulse duration of 100 fs, an energy of 900 μJ per pulse, and a repetition rate of 1 kHz. Ten percent of the amplified output was focused onto a 1.2 cm rotating quartz plate to generate a white light continuum, which was further split into two parts used as probe and reference beam, respectively. The rest of the CPA output was used to pump an optical parametric amplifier (IR-OPA, Clark-MXR), that was modified to generate excitation pulses at 460 nm through sum-frequency mixing. Excitation at 395 nm was obtained from the second harmonic generation of the CPA output. The pump pulse was sent through a translation stage (Compumotor, Rohnert Park, CA) to vary the time delay between the pump and the probe pulses. The excitation energy at the sample was 1 μJ per pulse at 460 nm, focused to a 0.5 mm spot, or 2.5 μJ per pulse at 395 nm with a larger spot size (1.5 mm in diameter). The polarization of the pump beam was set at the magic angle with respect to the probe and reference beams. The probe and reference beams were focused into a dual-leg optical fiber bundle coupled with a spectrograph (SP275, Acton Research, Acton, MA). Whole spectra (over a 140 nm range) were recorded at each time position using a dual diode array detector (ST121, Princeton Instrument, Trenton, NJ).

Data analysis

Dispersion correction and SVD analysis

At subpicosecond and picosecond times, the wavelength-dependent speed of light in condensed phase media results in a variation of signal onset time that is wavelength-dependent (absorbance changes in the blue region of the spectrum appear to occur before those in the red region). Time versus wavelength data sets, collected using both 395 nm excitation and 460 nm excitation, were corrected for this dispersion using a polynomial correction curve determined from multiexponential fits of the initial rise time as a function of wavelength, including deconvolution of the Gaussian instrumental response function (Freiberg et al., 1998). These data sets were subjected to single value decomposition (SVD) analysis. Only the first four time/wavelength vector pairs resulting from the fits showed a nonrandom time evolution, and were used for data fitting and analysis. All of these manipulations were performed by a locally written algorithm based on the MATLAB linear algebra program (Mathworks).

Data fitting

Nonlinear least-squares fits of the SVD-reconstructed time-dependent data between -1 ps and 7 ps over the 410–570 nm spectral region (at the representative excitation wavelengths) were performed using an implementation of the Levenberg-Marquardt algorithm (Press et al., 1992, pp. 681–688), provided as part of the Microcal Origin (Version 5.0) software package. The function used to fit the data consisted of a single exponential term for the decay in addition to a Gaussian cross-correlation function representing the pump and the probe laser pulses that incorporated the instrumental response function of the entire measurement system (Ujj et al., 1998). The cross-correlation time (CCT) measures the temporal behavior of the laser pulses (pulse widths) and the fluctuation of the temporal overlap of the pump and probe laser pulses (pulse jitter). The probe wavelengths were selected by means of spectral filtering of the femtosecond white light continuum. The CCT was found to be probe wavelength-dependent, and ranged from 0.5 to 0.9 ps. Femtosecond transient absorption (FTA) traces, at eight different wavelengths with 460 nm excitation and seven wavelengths with 395 nm excitation, were analyzed using the above-described global kinetic fit procedure. The Gaussian cross-correlation function and the single exponential decay term included in the model function were able to satisfactorily fit the entire FTA traces over the -1 to 7 ps delay time scale (see below). No remaining systematic residual term was found. This indicates that the excited state decay time of PYP can be extracted from the data with the available signal-to-noise ratio.

RESULTS

Time-resolved spectra

Transient absorption spectra between -1 and 7 ps over the 410–570 nm spectral region were recorded after excitation at either 395 or 460 nm. Such femtosecond time-resolved spectra allow one to characterize the kinetic processes of excited state absorption, ground state bleaching and recovery, and initial photoproduct appearance. Typical spectral data as a function of time (shown for 460 and 395 nm excitation in Fig. 1) demonstrate the presence of ground state bleaching in the 430–465 nm region and stimulated emission in the 500–550 nm region. These transient spectra are in good agreement with the ground state absorption (Meyer et al., 1987) and fluorescence emission spectra (Meyer et al., 1991) of PYP, as well as with previously published time-resolved spectral data (Ujj et al., 1998; Baltuška et al., 1997). Note that the stimulated emission observed with 395-nm excitation pulses extends significantly further to the red than is the case for 460-nm excitation. We will return to this below. In addition to these results, we have also obtained data at longer times (up to 500 ps; not shown) which have confirmed the previous observations (Ujj et al., 1998) of the formation of the I_0 and $I_0^{\ddagger}$ species.

The kinetic decay traces (examples shown in Fig. 2) at all observation wavelengths (probe wavelengths), and for both exciting wavelengths, show transient excited state formation occurring within a few hundred femtoseconds as a negative differential signal. The subsequent absorbance increase in the 430–460 nm region, which measures ground state recovery, was incomplete within the measuring time window for both excitations (Fig. 2), implying the formation of at least one other species upon decay of the excited state (presumably a photochemical product, i.e., I_0). The decay of stimulated emission was essentially complete on this time scale.

Global nonlinear least-squares fits of the data obtained with 460-nm excitation, illustrated in Fig. 2, *A* and *B* for both ground state bleaching wavelengths (410–460 nm) and stimulated emission/photochemical intermediate formation wavelengths (480–520 nm), demonstrate that the decay portion of the curves can be fitted well with a single exponential function with a k_{obs} value of $0.83 \pm 0.05 \times 10^{12}$ s^{-1} (see Table 1), at all of these probe wavelengths. Using 395-nm excitation, probing in the long wavelength region yields a similar rate constant (Fig. 2 *C*) ($k_{obs} = 0.91 \pm 0.01 \times 10^{12}$ s^{-1}; see Table 1), whereas a significantly

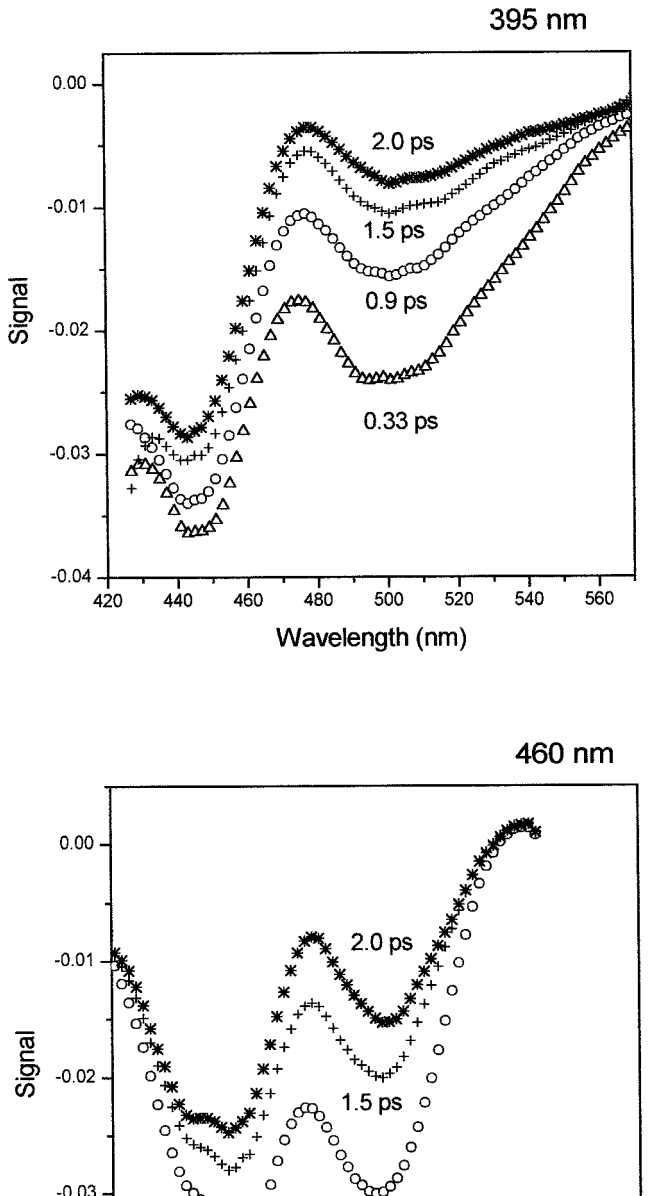

FIGURE 1 Femtosecond time-resolved difference spectra for excitation wavelengths 395 nm (*top*) and 460 nm (*bottom*) in the 427–570 nm spectral region; ground state repopulation occurs in the 420–470 nm region, and stimulated emission from 470 to 530 nm. Experimental data points after dispersion correction are shown at 0.33, 0.9, 1.5, and 2.0 ps times after excitation. A minor laser scattering artifact appears at ~458 nm in the bottom panel.

different rate constant ($k_{obs} = 0.50 \pm 0.07 \times 10^{12}\ s^{-1}$) was obtained probing in the short wavelength region. We will return to this latter point below.

The simplest kinetic model that can account for the incomplete repopulation of the ground state, and for the occurrence of a single wavelength independent decay rate constant, would involve two competing processes: 1) the repopulation of the ground state from the excited state, directly observed at 410–460 nm, and observed indirectly via stimulated emission at 480–520 nm (occurring with a rate constant k_d); 2) the formation of a single photochemical intermediate, I_0 (occurring with a rate constant k_p). This is shown in Fig. 3 by the pathway involving P* (the second pathway, involving P*′, will be discussed below). This hypothetical model predicts that generation of the photochemical species will compete with repopulation of the ground state, and thus the relative amounts of intermediate (I_0) and ground state PYP (P_{GS}) produced from P* (i.e., the quantum yield of photoproduct formation) will depend on the relative magnitudes of k_d^b and k_p^b (Fig. 3). Assuming no additional intermediates other than I_0 formed within the present 7-ps time window, we would expect to obtain decay curves with the same observed rate constant at all wavelengths, corresponding to $k_{obs} = k_d^b + k_p^b$, consistent with the single exponential decay ($k = 0.83 \times 10^{12}\ s^{-1}$) obtained at all wavelengths for the 460-nm data set.

Deconvolution of the rate constants k_d^b and k_p^b from k_{obs} can be accomplished as follows. From decay data obtained at 447 nm with 460 nm excitation (not shown), one can calculate the extent of "permanent" bleaching of the ground state (53%) after excited state decay is complete, and thus the partitioning of the excited state between the repopulation of the ground state and the formation of I_0 can be determined. This directly gives the ratio k_p^b/k_d^b. Since the value of $k_d^b + k_p^b$ ($=k_{obs}$) is already known, the individual rate constant values can be calculated. This yields $k_p^b = 0.34 \times 10^{12}\ s^{-1}$ ($\tau = 1.9$ ps) and $k_d^b = 0.29 \times 10^{12}\ s^{-1}$ ($\tau = 3.4$ ps) for the 460-nm data set (Table 1).

Similarly, for the 395-nm data set the extent of bleaching of the ground state after excited state decay was determined to be 60% at 447 nm (Fig. 2 *D*). For this data set, the k_{obs} value obtained upon analysis of the long wavelength data (470–530 nm) was similar to that obtained from 460-nm excitation at all observation wavelengths ($0.91 \pm 0.01 \times 10^{12}\ s^{-1}$; Table 1). Thus, the individual rate constant values calculated from k_{obs} are $k_d^b = 0.34 \times 10^{12}\ s^{-1}$ ($\tau = 2.9$ ps) and $k_p^b = 0.57 \times 10^{12}\ s^{-1}$ ($\tau = 1.8$ ps), as given in Table 1. We consider these to be, within experimental error, the same as those obtained with 460-nm excitation. However, for the 395-nm excitation data at shorter wavelengths (410–460 nm) a significantly smaller value of k_{obs} ($0.5 \pm 0.07 \times 10^{12}\ s^{-1}$) was obtained. For these data, we calculate the individual rate constants to be $k_p^a = 0.31 \times 10^{12}\ s^{-1}$ ($\tau = 3.2$ ps) and $k^b = 0.19 \times 10^{12}\ s^{-1}$ ($\tau = 5.3$ ps). As will be discussed below, these two rate constants correspond to the processes defined in Fig. 3, which proceed from an alternate excited state P*′.

The results of the global analyses of these data are shown by the solid lines through the data points in Fig. 2. Global fits encompassing other wavelengths also gave results consistent with these. As observed previously (Ujj et al., 1998), the I_0 intermediate can be kinetically observed at both short

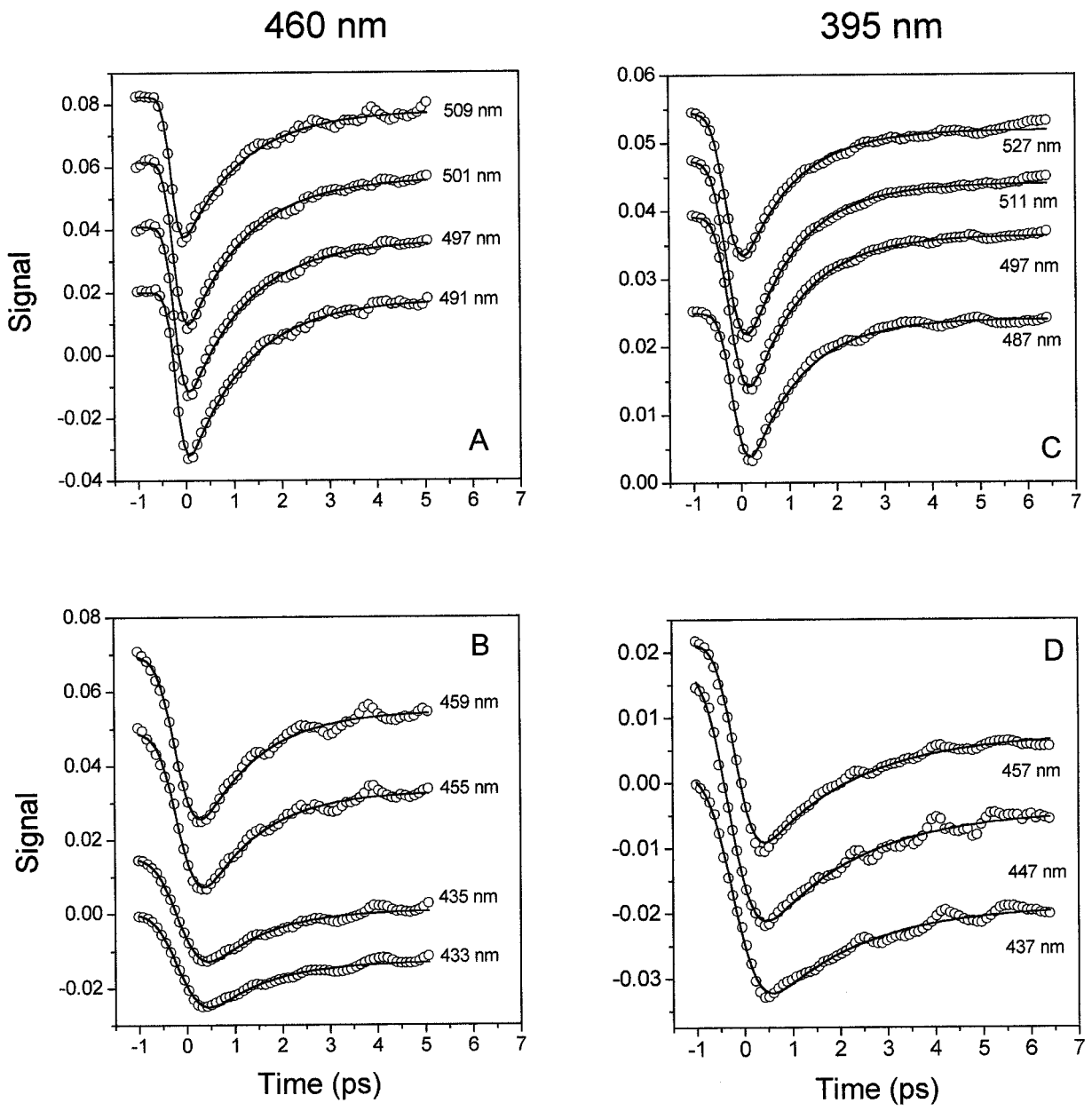

FIGURE 2 Kinetic traces obtained at several different wavelengths in the −1 to 7 ps time range. Curves are shifted vertically for clarity. Open circles represent the experimental data points for all the curves. *A* and *B* correspond to 460-nm excitation and *C* and *D* to 395-nm excitation. The solid lines through the data points represent the results of global analysis applied simultaneously to all the data sets using a single exponential equation for the decay portion of the curve (see text for details).

and long observation wavelengths, but is spectrally buried within the stimulated emission. It is important to note that the amplitude of the stimulated emission band for the 460-nm excitation data is significantly larger relative to that of the ground state bleaching signal than is the case for the 395-nm excitation data, and that the emission extends further to the red with 395 nm excitation. Furthermore, with 460 nm excitation, excited state decay is more rapid relative to the decay observed at shorter wavelengths for the 395 nm excitation (see values given in Table 1). These observations suggest that excitation at 395 nm leads to a different excited state population (designated as P*′ in Fig. 3) than that formed by 460 nm excitation (designated as P* in Fig. 3), resulting in an alternative photochemical pathway with different time constants (Fig. 3), which is only observed kinetically by probing at the shorter wavelengths. An alternate possibility is the existence of a nonhomogenous ground state population of PYP molecules, which are excited to different states at the two wavelengths. However, no evidence for such inhomogeneity is obtained from the ground state absorption spectrum of PYP and from kinetic data obtained on the slower time scales. The smaller rate constants observed with 395 nm excitation for the repopulation of the ground state ($k^b = 0.19 \times 10^{12}\ s^{-1}$) and the forma-

TABLE 1 Kinetic rate constants for 460 and 395 nm excitation obtained by global analysis

Rate constant	Short wavelengths (420–470 nm)	Long wavelengths (470–530 nm)
460-nm data		
k_{obs} ($k_d + k_p$)	$0.83 \pm 0.05 \times 10^{12}$ s^{-1} (1.2 ps)	$0.83 \pm 0.02 \times 10^{12}$ s^{-1} (1.2 ps)
k_d (repopulation of ground state)	0.29×10^{12} s^{-1} (k_d^b) (3.4 ps)	0.29×10^{12} s^{-1} (k_d^b) (3.4 ps)
k_p (photochemical product formation)	0.54×10^{12} s^{-1} (k_p^b) (1.9 *ps*)	0.54×10^{12} s^{-1} (k_p^b) (1.9 ps)
395-nm data		
k_{obs} ($k_d + k_p$)	$0.50 \pm 0.07 \times 10^{12}$ s^{-1} (2.0 ps)	$0.91 \pm 0.01 \times 10^{12}$ s^{-1} (1.1 ps)
k_d (repopulation of ground state)	0.19×10^{12} s^{-1} (k^b) (5.3 ps)	0.34×10^{12} s^{-1} ($k_d^a \sim k_d^b$) (2.9 ps)
k_p (photochemical product formation)	0.31×10^{12} s^{-1} (k_p^a) (3.2 ps)	0.57×10^{12} s^{-1} (k_p^b) (1.8 ps)

Note: In 460-nm data, $k_p/k_d = 0.53$; in 395-nm data, $k_p/k_d = 0.60$. Numbers in parentheses correspond to time constant values.

tion of the photochemical intermediate I_0 ($k_p^a = 0.31 \times 10^{12}$ s^{-1}) are ascribed to slower internal conversions from P*′ to the P* state and the I_0^* state, respectively. The latter species, which corresponds to an excited state of I_0, is introduced to account for the long wavelength component of the stimulated emission, shown in Fig. 1. The rate constant for the decay of the stimulated emission from this state (k_d^a) is approximately the same as the rate constant for the stimulated emission decay from P* (k_d^b), as shown by the parallel decay of the observed components of the stimulated emission in Fig. 1. Although the scheme shown in Fig. 3 can account for the present observations, it must be considered hypothetical at this point. Temperature dependence measurements and two-excitation pulse experiments studying excited states of I_0 should provide further insights into this mechanistic model. Such studies are underway.

DISCUSSION

As shown above, transient absorption changes probed on the subpicosecond time scale have kinetically revealed the rate constant for the formation of the recently reported picosecond intermediate I_0 (Ujj et al., 1998). At the time resolution of the measurements, no additional early intermediates preceding I_0 were apparent. Excitation at both the 395- and 460-nm wavelengths yield similar rise kinetics (probably limited by the pulse width of the laser) to form vertically excited Franck-Condon states. This would suggest excitation from a nonheterogenous population in the ground state potential energy surface (designated P_{GS} in Fig. 3). However, as noted above, the wavepacket in the excited state created by the absorption depends on the excitation wavelength. As the wavepacket moves away from the Franck-Condon region, the excited state absorption and the stimulated emission decrease with time either because of photochemical intermediate formation or reformation of the ground state. These processes are competitive. The time scale of decay of the excited state depends on the nature of the excited state that is formed (i.e., it is excitation wavelength-dependent, as shown in Table 1). From the transients shown in Fig. 2, it is possible to calculate the percentage return of the excited state to the ground state, and thus the quantum yield of formation of the first photochemical intermediate. Values of 0.5 ± 0.1 and 0.6 ± 0.1 were obtained for excitation at 460 and 395 nm, respectively. These are in satisfactory agreement with the previously reported value of 0.67 obtained from photobleaching measurements (Meyer et al., 1989) and with previous picosecond experiments (Ujj et al., 1998).

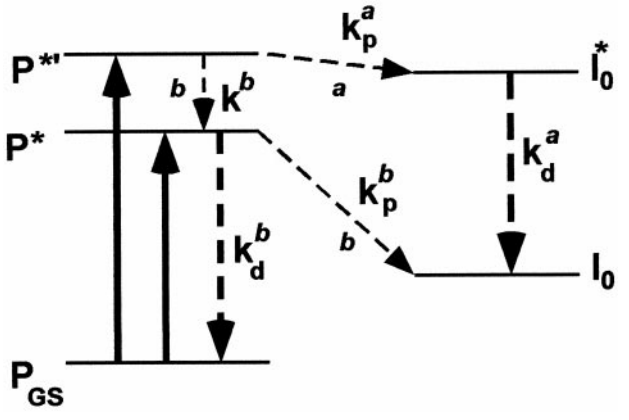

FIGURE 3 Kinetic model for excited state formation and decay and photochemical product formation from ground state (dark-adapted) PYP (P_{GS}). A 460-nm excitation produces excited-state P*, and 395-nm excitation produces P*′. Formation of the initial photochemical intermediate I_0 occurs along pathway *b* from P*, and from P*′ after relaxation (k^b) to P*, with a rate constant k_p^b. I_0 is also produced with a rate constant k_p^a from P*′ via I_0^* (an excited state of I_0), which is formed along pathway *a*. Stimulated emission decay occurs with rate constants k_d^a and k_d^b from the two excited states P* and I_0^*. Thin dashed lines indicate radiationless processes, whereas thick dashed lines correspond to decay processes that can occur radiatively and which result in stimulated emission.

The difference in the nature of the excited states formed at the two excitation wavelengths located on the long and short wavelength sides of the PYP absorption band reflects a complex behavior during the excitation pulse and can probably be attributed to differences in the vibrational and conformational properties of the excited state potential surfaces, as well as to the dynamic properties of the excited state resulting from the spreading or movement of the wavepacket on the potential energy surface as it leaves the Franck-Condon region. This may reflect a change in the coupling between the various torsional or vibrational modes of the chromophore within the excited state population generated by 395 nm excitation. In fact, there appears to be a small oscillatory component to some of the kinetic traces in Fig. 2, particularly when 460 nm excitation is used. At present, the signal-to-noise level in the data does not allow an unambiguous interpretation of this signal, but in princi-

ple, information about the coupling of reaction dynamics to specific low-frequency vibrations may be derived from more detailed measurements and analyses of long-lived oscillations such as these. Experiments to address these issues are in progress.

CONCLUSIONS

Using femtosecond time-resolved absorption spectroscopy we have been able to evaluate the rate constants for repopulation of the ground state and formation of the first photochemical intermediate from the excited state of PYP. In addition, we have shown that there are no additional intermediates formed within the time resolution of the present experiment.

Photoisomerizations are known to be rapid processes, which occur as a result of the absorption of a high-energy photon (Schoenlein et al., 1991). In PYP, structural changes on the femtosecond time scale are probably restricted to the chromophore itself within the closely packed hydrophobic binding pocket, and consequent changes in the protein environment are thermally driven and slower. The first event observed in the PYP photocycle has been ascribed to the breaking of the hydrogen bond between the carbonyl oxygen of the covalent thiol ester and the backbone amide hydrogen of Cys-69, along with a partial twist of this thioester bond, by a 0.85 Å resolution crystallographic determination of the structure of an intermediate trapped at −100°C (Genick et al., 1998). This photogenerated structure clearly shows a 166° rotation of the thioester carbonyl bond relative to the phenolic ring, whereas the olefinic double bond has been minimally converted from the *trans* to the *cis* conformation. The distorted transition state-like geometry of this intermediate has been postulated to cause subsequent larger, more slowly occurring, movements associated with the complete isomerization about the C═C bond attached to the phenolic ring. It is possible that the I_0 intermediate observed in this and the previous study (Ujj et al., 1998) corresponds to this thioester carbonyl rotated species, with the distorted geometry of the chromophore also depending on the specific intramolecular vibrational energy redistribution resulting from the position of the wavelength of excitation with respect to the PYP absorption band. The thioester bond twist would then correspond to the initial minimal movement in the photochemical pathway driven by the absorption of light energy, thereby forming a transient, but kinetically observable, species. The revised photocycle of PYP is presented in Fig. 4. We presume that the twist of the thiol ester bond facilitates the completion of the *trans-cis* isomerization of the chromophore, and as a consequence of this the protein environment around the chromophore undergoes conformational changes, whereby the chromophore breaks its H-bonds to Tyr-42 and Glu-46, and with Arg-52 moves out into the solvent to pick up a proton ($I_1 \rightarrow I_2$), forming the fully bleached, blue-shifted intermediate (Meyer et al., 1993; Genick et al., 1997b, 1998; Ujj et al., 1998).

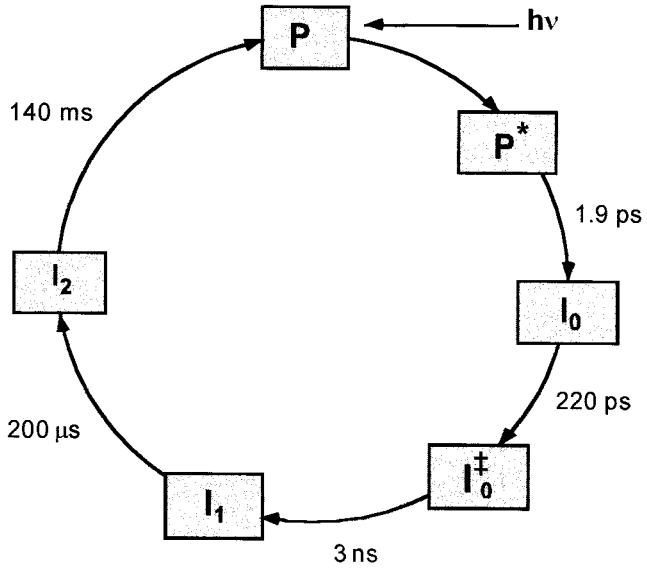

FIGURE 4 Revised PYP photocycle.

Although the chromophore and protein structures are quite different, the kinetic behavior of the photocycles of PYP and the rhodopsin family, i.e., fast photoisomerization and the formation of spectroscopically distinct intermediates, is similar. The mechanistic models proposed for these photoactive proteins are also similar: namely, the formation of early (red-shifted) intermediates involving vibrational and/or twisting movements restricted to the chromophore, on the femtosecond and subpicosecond time scales (Nuss et al., 1985; Schoenlein et al., 1991; Lewis and Kliger, 1992; Wang et al., 1994). The photon energy is briefly stored in these distorted structures, resulting in the generation of additional slower intermediates, thereby completing transduction of the biological signal.

We are grateful to Drs. Zdzislaw Salamon and Terry Meyer for assistance with the preparation of this manuscript.

This work was supported by National Science Foundation Grants MCB-9722781 and MCB-9513457.

REFERENCES

Baca, M., G. E. O. Borgstahl, M. Boissinot, P. M. Burke, D. R. Williams, K. A. Slater, and E. D. Getzoff. 1994. Complete chemical structure of photoactive yellow protein: novel thioester linked 4-hydroxycinnamyl chromophore and photocycle chemistry. *Biochemistry.* 33: 14369–14377.

Baltuška, A., I. H. M. van Stokkum, A. Kroon, R. Monshouwer, K. J. Hellingwerf, and R. van Grondelle. 1997. The primary events in the photoactivation of yellow protein. *Chem. Phys. Lett.* 270:263–266.

Chosrowjan, H., N. Mataga, N. Nakashima, Y. Imamoto, and F. Tokunaga. 1997. Femtosecond-picosecond fluorescence studies on excited state dynamics of photoactive yellow protein from *Ectothiorhodospira halophila. Chem. Phys. Lett.* 270:267–272.

Devanathan, S., U. Genick, E. D. Getzoff, T. E. Meyer, M. A. Cusanovich, and G. Tollin. 1997. Preparation and properties of a 3,4-dihydroxycin-

namic acid chromophore variant of the photoactive yellow protein. *Arch. Biochem. Biophys.* 340:83–89.

Freiberg, A., K. Timpmann, S. Lin, and N. W. Woodbury. 1998. Exciton, relaxation and transfer in the LH2 antenna network of photosynthetic bacteria. *J. Phys. Chem.* 102:10974–10982.

Genick, U. K., G. E. O. Borgstahl, K. Ng, Z. Ren, C. Pradervand, P. M. Burke, V. Srajer, T. Teng, W. Schildkamp, D. E. McRee, K. Moffat, and E. D. Getzoff. 1997b. Structure of a protein photocycle intermediate by millisecond time-resolved crystallography. *Science.* 275:1471–1475.

Genick, U. K., S. Devanathan, T. E. Meyer, I. L. Canestrelli, E. Williams, M. A. Cusanovich, G. Tollin, and E. D. Getzoff. 1997a. Active site mutants implicate key residues for control of color and light cycle kinetics of photoactive yellow protein. *Biochemistry*. 36:8–14.

Genick, U. K., M. S. Soltis, P. Kuhn, I. L. Canestrelli, and E. D. Getzoff. 1998. Structure at 0.85 Å resolution of an early protein photocycle intermediate. *Nature*. 392:206–209.

Lewis, J. W., and D. S. Kliger. 1992. Photointermediates of visual pigments. *J. Bioenerg. Biomembr.* 24:201–210.

Meyer, T. E. 1985. Isolation and characterization of soluble cytochromes, ferredoxins and other chromophoric proteins from the halophilic phototrophic bacterium *Ectothiorhodospira halophila. Biochim. Biophys. Acta.* 806:175–183.

Meyer, T. E., M. A. Cusanovich, and G. Tollin. 1993. Transient proton uptake and release is associated with the photocycle of the photoactive yellow protein from the purple phototrophic bacterium, *Ectothiorhodospira halophila*. *Arch. Biochem. Biophys.* 306:515–517.

Meyer, T. E., J. C. Fitch, R. G. Bartsch, G. Tollin, and M. A. Cusanovich. 1990. Soluble cytochromes and a photoactive yellow protein isolated from the moderately halophilic purple phototrophic bacterium, *Rhodospirillum salexigens*. *Biochim. Biophys. Acta.* 1016:364–370.

Meyer, T. E., G. Tollin, T. P. Causgrove, P. Cheng, and R. E. Blankenship. 1991. Picosecond decay kinetics and quantum yield of fluorescence of the photoactive yellow protein from the halophilic purple phototrophic bacterium, *Ectothiorhodospira halophila*. *Biophys. J.* 59:988–991.

Meyer, T. E., G. Tollin, J. H. Hazzard, and M. A. Cusanovich. 1989. Photoactive yellow protein from the purple phototrophic bacterium *Ectothiorhodospira halophila:* quantum yield of photobleaching and effects of temperature, alcohols, glycerol, and sucrose on kinetics of photobleaching and recovery. *Biophys. J.* 56:559–564.

Meyer, T. E., E. Yakali, M. A. Cusanovich, and G. Tollin. 1987. Properties of a water-soluble, yellow protein isolated from a halophilic phototrophic bacterium that has photochemical activity analogous to sensory rhodopsin. *Biochemistry*. 26:418–423.

Nuss, M., W. Zinth, W. Kaiser, E. Kölling, and D. Oesterhelt. 1985. Femtosecond spectroscopy of the first events of the photochemical cycle in bacteriorhodopsin. *Chem. Phys. Lett.* 117:1.

Press, W. H., S. A. Teukolsky, W. T. Vetterling, and B. P. Flannery. 1992. Numerical Recipes in C: The Art of Scientific Computing, 2nd ed. Cambridge University Press, Cambridge, U.K. 59–70; 681–688.

Schoenlein, R. W., L. A. Peteanu, R. A. Mathies, and C. V. Shank. 1991. The first step in vision: femtosecond isomerization of rhodopsin. *Science*. 254:412–415.

Sprenger, W. W., W. D. Hoff, J. P. Armitage, and K. J. Hellingwerf. 1993. The eubacterium *Ectothiorhodospira halophila* is negatively phototactic, with a wavelength dependence that fits the absorption spectrum of the photoactive yellow protein. *J. Bacteriol.* 175:3096–3104.

Ujj, L., S. Devanathan, T. E. Meyer, M. A. Cusanovich, G. Tollin, and G. H. Atkinson. 1998. New photocycle intermediates in the photoactive yellow protein from *Ectothiorhodospira halophila*: picosecond transient absorption spectroscopy. *Biophys. J.* 75:406–412.

Wang, Q., R. W. Schoenlein, L. A. Peteanu, R. A. Mathies, and C. V. Shank. 1994. Vibrationally coherent photochemistry in the femtosecond primary event of vision. *Science*. 266:422–424.